Palladium nanoparticles stabilized by polyethylene glycol: Efficient, recyclable catalyst for hydrogenation of styrene and nitrobenzene

F.A. Harraz [a,*], S.E. El-Hout [a], H.M. Killa [b], I.A. Ibrahim [a]

[a] Nanostructured Materials and Nanotechnology Division, Central Metallurgical Research and Development Institute (CMRDI), P.O. 87 Helwan, Cairo 11421, Egypt
[b] Faculty of Science, Zagazig University, Egypt

ABSTRACT

We developed an efficient, simple chemical reduction method to produce highly active palladium (Pd) nanoparticles in polyethylene glycol (PEG) with no other stabilizer. The as-prepared Pd/PEG catalyst demonstrated a remarkable catalytic activity toward hydrogenation of both styrene and nitrobenzene under mild conditions. The Pd-PEG catalyst could be easily removed from the reaction mixture and its recyclability with no loss of activity was possible for seven times in case of styrene and three cycles for nitrobenzene. The catalytic performance was found to depend essentially on the catalyst and target concentrations and the reaction time. The catalyst was fully characterized by a variety of techniques including X-ray diffraction (XRD), transmission electron microscopy (TEM), UV–vis spectroscopy, Fourier transform infrared (FT-IR) spectroscopy, and N_2 adsorption–desorption isotherm. The reactivity of the Pd/PEG catalyst toward hydrogenation reactions is attributed to the high degree of dispersion of Pd(0) nanoparticles in PEG with small average particle size distribution of 5 nm. Results of the synthesis and characterization of Pd/PEG catalyst and its catalytic performance for hydrogenation reactions are presented and thoroughly discussed.

© 2011 Elsevier Inc. All rights reserved.

1. Introduction

Transition-metal nanoparticles science is a strategic research area in material development due to their particular physical and chemical properties and its diverse application fields including catalysis, photochemistry, electronics, optics, and magnetism [1–9]. Particularly for catalysis applications, palladium (Pd) nanoparticles is a unique class of heterogeneous catalysts that is widely used and effective for a variety of organic reactions due to its high surface-to-volume ratio. However, active surface atoms often led to aggregation of Pd(0) nanoparticles (Pd black), and hence the catalytic activity and selectivity would decrease. Therefore, it is an essential task to stabilize the nanoparticles for effective utilization. Various supports have been developed to stabilize Pd nanoparticles, including mesoporous silica support [10,11], surfactants [12,13], dendrimers [14,15], ionic liquids [16,17], block copolymer [18], and polyvinylpyridine [19]. In a recent report, Siamaki et al. reported a microwave-assisted method to generate active Pd nanoparticles supported on graphene for carbon–carbon cross-coupling reactions [20]. In another work, Wu et al. used polyphenol-grafted collagen fibers to stabilize the Pd nanoparticles [21]. Different inorganic materials, such as hydrotalcite, MgO, zeolite Beta, and γ-Al_2O_3 have also been utilized as effective supports for Pd nano-

particles [22,23]. It should be noted, however, that the choice of a suitable support is crucial because the interaction with the active phase plays a critical role during the catalytic reactions [24]. The main recorded disadvantages of the above supports are either its complexity or high cost, some are not environmentally accepted media, and poor selectivity and recyclability are sometimes observed. Therefore, it is desirable to develop Pd nanoparticles based catalytic systems supported/dispersed on a suitable mobile phase that are active, selective, stable, nonhazardous, and recyclable.

Metal-polymer based catalysts, on the other hand, are efficient category of catalysts as they have advantages over traditional catalysts including: large surface areas of the metal particles, effective stabilization of the nanoparticles, possible control of particle shape and size by varying the nature of the polymer, and the presence of polymer layers on the metal particles can improve the catalytic selectivity [25]. Polyethylene glycol (PEG) is a promising candidate to serve as soluble polymeric support. This particular choice of PEG is justified by its capability to act as both reducing agent and stabilizer to prevent the agglomeration and precipitation of particles in the solution [26]. In addition, PEG is inexpensive, nontoxic, and its properties can be tuned by simply changing molecular weight [27]. PEG is benign that is already approved for use in food industry. These features make it ideal stabilizer for synthesis of Pd nanoparticles, and therefore PEG can combine the advantages of both homogeneous and heterogeneous catalysis.

* Corresponding author. Fax: +202 25010 639.
  E-mail address: fharraz@cmrdi.sci.eg (F.A. Harraz).

Generally, there are four main synthetic approaches for preparation of catalysts [28]: (i) transition metal salt reduction, (ii) thermal decomposition and photochemical methods, (iii) ligand reduction and displacement from organometallics, and (iv) metal vapor synthesis, in addition to the electrochemical synthesis approach [29]. Among the aforementioned methods, the chemical reduction method that involves the reduction of corresponding metal salts with suitable reducing agents is merely one of the most cost-effective, since it requires simple equipment to produce the metallic nanoparticles [30].

Pd nanopartciles based catalytic systems are increasingly investigated by several research groups and being used in various organic transformations. For example, Corma et al. used both PEG and imidazolium ionic liquids as solvents for developing a homogeneous and reusable Pd catalytic system for the Suzuki, Sonogashira, and Heck reactions [31,32]. A ligand-free Heck reaction has been also catalyzed by in situ-generated Pd nanopartciles in PEG-400 as reported by Jin and co-workers [33]. As recent works of de Souza et al. [34] and Wang and co-workers [35], Suzuki–Miyaura cross-coupling reactions have been catalyzed efficiently using Pd/PVP and Pd/PEG as catalysts under various conditions. Li et al. used functionalized PEG supported Pd nanoparticles as a catalyst for aerobic oxidation of alcohols [36]. A series of novel benzazepines has been synthesized using a phosphine-free Pd-catalyzed Heck reaction in PEG polymeric support [37], in addition organostannoxane-supported Pd nanopartciles have been recently developed for Heck-coupling reactions [38].

Of particular importance of Pd/PEG catalytic systems, there are some precedents reporting the synthesis of Pd nanoparticles in PEG [26,39,40]. Pillai et al. carried out selective hydrogenation of olefins using phenanthroline stabilized Pd nanoparticles in PEG [39]. Luo et al. used PEG with different chain lengths to generate Pd nanoparticles catalyst for Heck reaction [26]. Here, the most prominent synthetic characteristic of the catalyst is the use of PEG alone without using any additional ligands. Following the procedure of Luo et al., Pd nanoparticles catalyst has been recently synthesized in PEG and used for the hydrogenation of different types of olefins [40]. However, a definite understanding of the limits of Pd/PEG catalyst formation and its morphology control is still lacking. To better understand the conditions necessary for generating such a catalytic system using a similar method as that proposed by Luo et al., a detailed investigation was conducted in which the catalyst phase and morphology were correlated to systematic variation in operating parameters. The effects of controlling reaction parameters such as Pd loading, effect of using different molecular weights of PEG (400–6000), the operating temperature, and the reaction time have been investigated in detail in this work.

In heterogeneous catalysis, the progressive deactivation of catalysts is a major economic concern and mastering their stability has become as essential as controlling their activity and selectivity. For that reason, there is a strong motivation to develop new cheaper and cleaner approaches for synthesizing catalysts that are stable and recyclable and to understand the mechanisms leading to any loss in activity and selectivity. Accordingly, the second main objective of the present work is to examine/describe in details the catalytic performance of as-synthesized Pd/PEG catalysts for the hydrogenation of styrene and nitrobenzene as two reaction models under mild conditions. Hydrogenation of C═C double bonds is of significant importance due to great demands in chemical, petrochemical, pharmaceutical, and food industries [40]. The catalytic hydrogenation of nitrobenzene, on the other hand, is an industrially important reaction for the production of aniline, which is an important intermediate for polyurethanes, dyes, pharmaceuticals, explosives, and agricultural products [41].

In this work, we show that the ideal green catalytic process of "one-phase catalysis and two-phase separation" for both hydrogenation reactions could be achieved in this study, because the reactants are miscible in PEG, while the products are immiscible. Therefore, pure final products could be separated by simple decantation. The catalytic performance of both systems is evaluated and will be thoroughly addressed.

2. Experimental

2.1. Preparation of Pd nanoparticles

The procedure was adapted to that reported by other authors [26]. Pd(II) acetate [$(CH_3COO)_2Pd$] Aldrich with 99.9% purity was added into PEG with different molecular weights (400, 800, 1000, 2000, 4000, and 6000) in a 50-ml round-bottomed flask. Different wt.% of Pd acetate/ PEG, mainly 1.2%, 2.5%, 3.75% and 4.8%, were essentially used. The mixture was heated in a water bath at 75 °C under vigorous, continuous stirring for 2 h. During this stage, the light yellow color of the solution turned brown and finally to gray dark, indicating the formation of Pd nanoparticles. The mixture of Pd nanoparticles in PEG solidified upon cooling at room temperature.

2.2. Characterization of Pd/PEG catalyst

Phase identification and crystallite size measurements of Pd nanoparticles were performed by X-ray diffraction (XRD, Bruker AXS D8 Advance, Germany) with Cu$k\alpha$ radiation (λ = 1.5406 Å). Measurements were taken with a tube power of 40 kV and 40 mA, from 10° to 80° 2θ, with a 0.02° 2θ step size and 0.4 s count time. The specific surface area (S_{BET}), pore volume, and pore size distribution of the samples were determined by surface area and pore size analyzer (QUANTACHROME-NOVA 2000 Series, UK). For detailed morphological and structural analysis, an JEOL JEM-1230 transmission electron microscope (TEM) operating at 200 kV was used. Selected-area electron diffraction (SAED) patterns for some prepared catalysts were also recorded. Before TEM observation, the samples were first prepared by dispersing a trace amount of the catalyst in ethanol followed by ultrasonic vibration for 20 min. A carbon film coated copper grid was then quickly immersed into the dispersion and left in air for drying. UV–vis spectroscopy measurements (V570 spectrophotometer Jasco Co.) were performed for Pd(II) ions before and after reduction with PEG. FT-IR spectra were measured for as-prepared catalyst by means of 3600 JASCO spectrophotometer. The spectra were collected over the frequency range of 4000–400 cm^{-1}.

2.3. Hydrogenation reactions

Hydrogenation of styrene and nitrobenzene was conducted in liquid phase in a 50-ml round-bottomed flask equipped with a reflux condenser and a magnetic stirrer. In a typical reaction procedure, known concentrations of the target compound, 1 mmol of biphenyl as standard and a certain weight of the Pd/PEG catalyst were mixed in 20 ml of absolute ethanol as a solvent, stirring and heating the mixture for 4 h at room temperature in hydrogen atmosphere. After the reaction, the mixture was extracted with diethyl ether and analyzed by Agilent GC 7890A model: G3440A Gas Chromatography using 19091J-413 capillary column (30 m × 320 μm × 0.25 μm). Chromatographic conditions applied for hydrogenation of styrene and nitrobenzene are summarized in Table 1. In the catalyst recycling experiments, the reaction mixture was cooled to room temperature, and the organic products were extracted into diethyl ether and finally removed by a simple decantation. The Pd/PEG catalyst is immiscible in ether and could be easily recovered and used for the next reaction cycle. The

Table 1
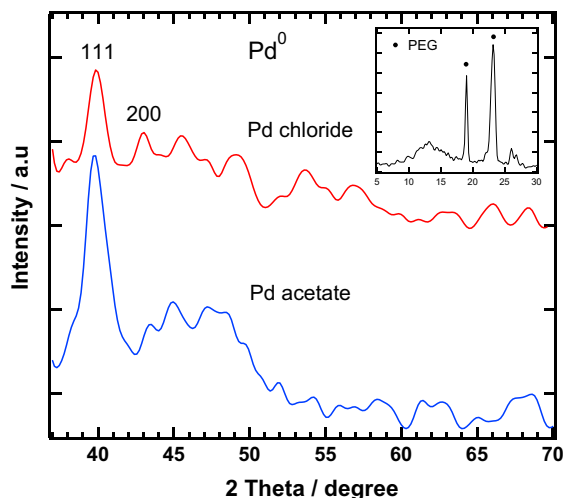Chromatographic conditions applied for hydrogenation of styrene and nitrobenzene.

	Hydrogenation of styrene	Reduction of nitrobenzene
Oven	60 °C for 3 min → 200 °C	50 °C for 5 min → 200 °C for 1 min
	60 → 200 °C 10 °C/min	50 → 200 °C 10 °C/min
Detector	Type: FID	Type: FID
	Heater: 300 °C	Heater: 300 °C
	H_2 flow: 35 ml/min	H_2 flow: 30 ml/min
	Air flow: 400 ml/min	Air flow: 400 ml/min
	Makeup flow: 20 ml/min	Makeup flow: 25 ml/min
Injection	Heater: 250 °C	Heater: 250 °C
	Pressure:10 psi	Pressure:13.762 psi
	Total flow: 93.099 ml/min	Total flow: 41.384 ml/min
	Septum purge flow: 3 ml/min	Septum purge flow: 3 ml/min
	Mode: split with ratio (40:1)	Mode: split with ratio (10:1)
Column	30 m × 320 μm × 0.25 μm	30 m × 320 μm × 0.25 μm

Fig. 2. UV–vis spectra of palladium acetate and Pd/PEG4000 catalyst.

extracted Pd content was analyzed by an inductively coupled plasma-optical emission spectrometer (ICP-OES) model Perkin/Elmer Optima 2000. Photographs of recycling procedure are provided in Supporting information (Fig. S1).
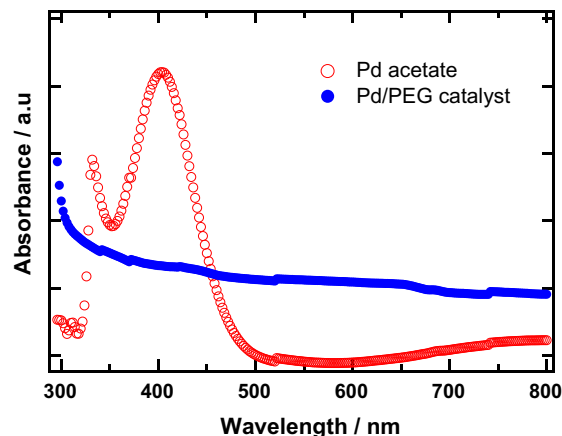
3. Results and discussion

3.1. Characterization of Pd/PEG catalyst

Upon addition of Pd(II) acetate into PEG4000 with a 3.75 wt.% (Pd(II) acetate 0.15 g (0.67 mmol)/ PEG 4 g (1 mmol) under vigorous stirring at 75 °C for 2 h, the chemical reduction of Pd(II) ions with PEG resulted in the *in situ* formation of Pd(0) nanoparticles that were still stabilized by PEG matrix. Herein, PEG serves as both a reducing agent and a stabilizer for the Pd(0) nanoparticles. The crystalline structure of as-synthesized catalyst was obtained using powder XRD. The typical patterns of catalysts prepared using Pd(II) acetate and Pd(II) chloride in PEG4000 are presented in Fig. 1. The inset shows two peaks at about 19.2° and 23.4° indicating the presence of pure PEG polymer [42]. As shown in the XRD patterns, broad peak near $2\theta = 40°$ is detected, which can be indexed to the characteristic reflection (1 1 1) plane for face-centered-cubic Pd(0) with another weak peak around $2\theta = 43°$, consistent with the (2 0 0) crystalline plane (JCPDS card No. 87–641, $d = 2.28$,

1.97, respectively). No significant change of the diffraction pattern was observed upon changing the Pd(II) precursor, except the relatively more intense peak obtained in case of using Pd(II) acetate, which probably related to the different degree of chemical reduction of both Pd salts in PEG. The reflection peak shapes are broader than that of bulk Pd, indicating that Pd(0) is highly dispersed into PEG with small crystallite size. The crystallite size was calculated using Scherer's equation, and the value corresponding to the reflection plane (1 1 1) was found to be 3 nm.

To ensure the complete reduction of Pd(II) ions, UV–vis spectra of Pd(II) acetate before and after reduction with PEG4000 was measured, and the recorded spectra are shown in Fig. 2. As can be seen, the UV–vis spectrum of Pd(II) acetate shows absorption maximum at around 400 nm, which is characteristic of Pd(II) ions [26,43]. After the reaction of Pd(II) ions in PEG4000, the peak observed at 400 nm disappeared, indicating the complete conversion of Pd(II) to Pd(0) nanoparticles.

The morphology of as-prepared catalyst was further observed with TEM. The recorded image is shown in Fig. 3 with the SAED pattern and particle size distribution depicted in the inset. The TEM image visualized the presence of narrow size distributed spherical Pd nanoparticles. It can be seen that the average dimension of Pd nanoparticles fabricated at 75 °C using PEG4000 is around 4 nm, in good agreement with the crystallite size calculated from XRD data. The SAED pattern shown in the inset exhibits the

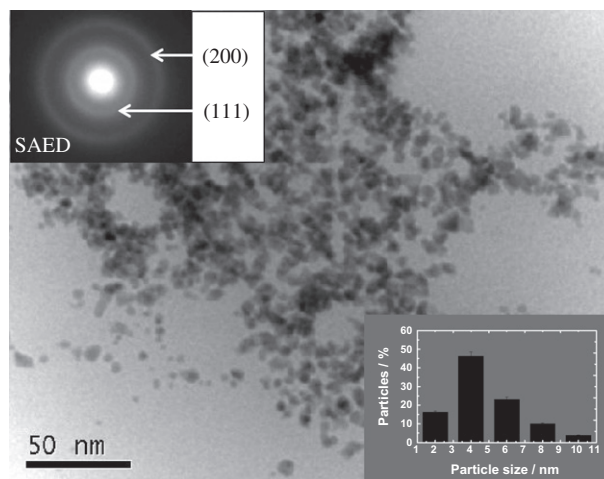**Fig. 1.** XRD for Pd nanoparticles prepared by different Pd sources. The inset is related to the pattern of PEG.

Fig. 3. TEM image of Pd nanoparticles in PEG4000 with 3.75 wt.%. Particle size distribution for Pd/PEG4000 (3.75%) and the SAED pattern are shown in the inset.

Table 2
Textural properties from N_2 adsorption–desorption isotherm measurements of Pd/PEG4000 catalysts prepared using different wt.% of Pd(II)/PEG.

Sample	BET [a] (m^2/g)	MicroPA [b] (m^2/g)	MicroPV [c] (cc/g)	Total PV [d] (cc/g)	Average PD [e] (nm)	MicroPW [f] (nm)
Pd/PEG (1.2%)	11.38	21.72	0.00766	0.00294	1.072	35.71
Pd/PEG (2.5%)	70	133.62	0.0471	0.0181	6.6	219.64
Pd/PEG (3.75%)	112.75	215.22	0.0759	0.0291	10.62	353.77
Pd/PEG (4.8%)	10.97	20.94	0.00739	0.00283	1.033	34.42

[a] BET surface area calculated from the linear part of the BET plot.
[b] Micropore area.
[c] Micropore volume.
[d] Total pore volume, taken from the volume of N_2 adsorbed at about $p/p° = 1$.
[e] Average pore diameter.
[f] Micropore width.

(1 1 1) and (2 0 0) directions confirming again the cubic structures and the crystalline nature of the catalyst, in consistent with XRD result of Fig. 1. The TEM analysis implies that the long-chain structure of PEG could provide good stability and dispersing effects to the Pd nanoparticles and prevent its agglomeration.

The formation of Pd(0) nanoparticles by a thermal heating of Pd precursor in the presence of PEG without adding any further reducing agent may proceed through the oxidation of the hydroxyl group (O—H) in PEG chains. The FTIR analysis of PEG after the reaction with Pd(II) ions revealed a new absorption peak appeared at around 1739 cm^{-1}, which could be attributed to the formation of aldehyde group (—CHO) during the reduction of Pd(II) ions (see Fig. S2 of Supporting information). This is actually in agreement with a similar analysis done by ^{1}H NMR and confirmed the formation of aldehyde group for a similar reaction system [26].

3.2. Influence of Pd loading, temperature, reaction time, and PEG molecular weight on as-formed Pd nanoparticles

To better understand the conditions necessary for the formation of Pd nanoparticles in PEG matrix, series of experiments were

Table 3
Crystallite size for Pd/PEG prepared at different temperatures and different times.

Temperature (°C)/time (h)	Crystallite size (nm)	BET (m^2/g)
50/2	–	–
75/2	3	112.75
100/2	7.7	82.7
125/2	7.7	70
150/2	–	–
75/1	9.4	–
75/3	6.3	66.2
75/4	6.9	–

further conducted in which the phase formation, particle size, and morphology were correlated to systematic variation in operating parameters.

Different Pd loading/ wt.% of Pd acetate/PEG (1.2%, 2.5%, 3.75%, and 4.8%) were used to investigate the evolution of Pd nanoparticles morphology and surface area. All samples were synthesized at 75 °C for 2 h. The BET surface area (S_{BET}) and pore parameters of Pd/PEG4000 synthesized using different wt.% are summarized in Table 2. The results reveal that the surface area of as-formed catalyst remarkably increased from 11.4 to 112.8 m^2/g by increasing
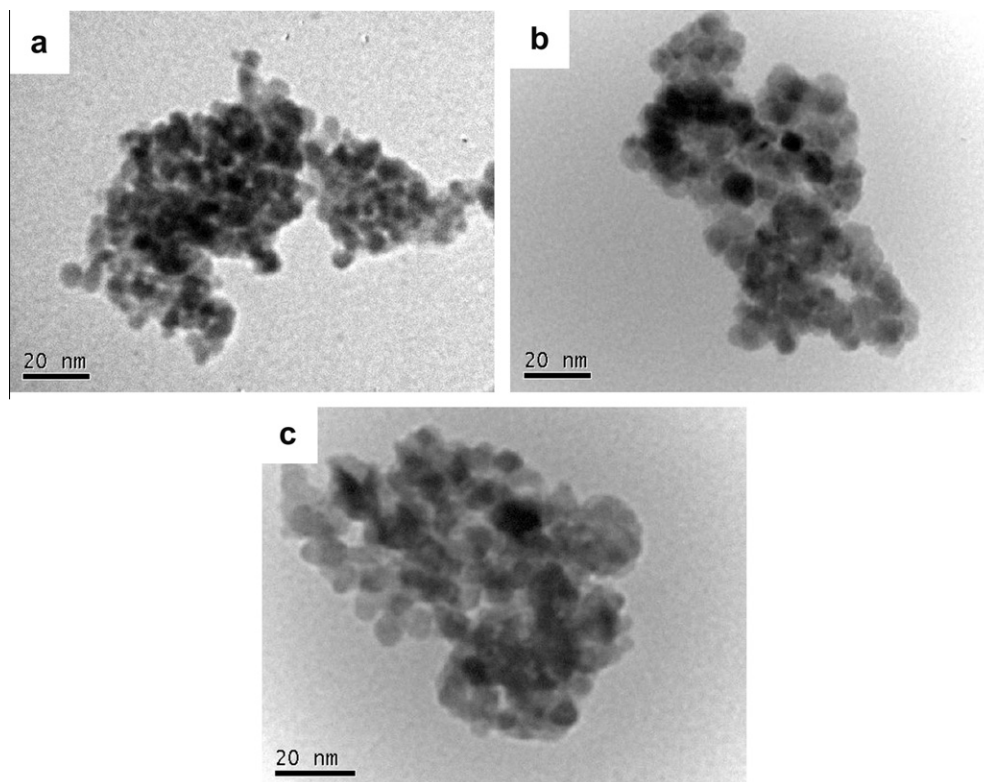
Fig. 4. TEM images of Pd nanoparticles in PEG4000 prepared at different temperatures: 75 °C (a); 100 °C (b); 125 °C (c).

Pd(II) acetate/PEG wt.% from 1.2% to 3.75%, whereas the surface area dropped again with further increase in wt.%. The maximum S_{BET} and total pore volume were achieved at 3.75 wt.%. This result is likely due to that the Pd/PEG wt.% affected the rate of chemical reduction of Pd(II) ions by PEG as well as the coalescence degree of as-formed Pd particles, which in turn controlled the particle size and surface area of as-formed catalyst.

Reaction temperature and duration are also key operating parameters during the thermal heating process of the reduction of Pd(II) ions with PEG. Experiments using 3.75 wt.% and operating at different temperatures—50, 75, 100, 125, and 150 °C—and at different times—1, 2, 3 and 4 h—were conducted. Table 3 shows the dependence of crystallite size and surface area of as-synthesized Pd/PEG4000 catalyst on temperature and time. It is worthy to note that appropriate reaction time is necessary for obtaining an efficient reduction of Pd(II) ions in PEG, which finally led to the desired particle size and surface area of as-formed catalyst. Under the present conditions, complete reduction of Pd(II) is likely achieved after 2 h reaction duration. The finding indicates also that at 50 °C, the chemical reduction of Pd(II) ions was not initiated or the reaction itself is a very slow process at such low temperature. To speed up the reduction of Pd(II) by PEG, the reaction temperature was increased to 75 °C. Pd(0) nanoparticles with good dispersion, small crystallite size and high S_{BET} were accordingly formed. However, by increasing the temperature above 75 °C, the crystallite sizes increased with a consequence decrease in surface area, which may be related to some degree of particle sintering. It has been reported that the reduction in the specific surface area is related to the reduction of energy associated with the interface between particles and environment as a thermally activated natural phenomenon [44]. Another possibility is due to a decrease in pore volume of the samples with a temperature rising, and hence the surface area is expected to decrease. Examples of these catalyst products are presented in TEM images of Fig. 4. One can see that spherical Pd nanoparticles with average particle size 5 nm are obviously visible in the polymeric matrix in the sample prepared at 75 °C, Fig. 4a, compared to other samples prepared at 100 °C or 125 °C, Fig. 4b and c, respectively. In addition, the separation of Pd nanoparticles prepared at 75 °C was easier than those prepared at higher temperature. This may be a consequence of the good stability effect of PEG to the Pd nanoparticles at lower temperatures [26].

We also examined the effect of different PEG molecular weights (400, 800, 1000, 2000, 4000, and 6000) on the formation of Pd/PEG catalyst. It is an experimental fact in this study that the reactivity or reducing power of PEG was found to be a function of its average molecular weight. No reaction was observed, under the current experimental conditions, using PEG with low molecular weights of 400, 800, or 1000. Pd nanoparticles were partially developed in PEG2000. A complete conversion of Pd(II) ions to Pd(0) was achieved in PEG4000 and 6000. Fig. 5 displays the TEM images taken for as-formed Pd nanopartciles prepared in PEG2000 and 6000 using the same Pd/PEG wt.% at 75 °C for 2 h. Small particle size with high particle density and good dispersion of Pd(0) nanoparticles can be observed in case of using larger chain length of PEG6000, Fig. 5 image b. This is indicative of rapid, easier reduction of Pd(II) to Pd nanoparticles in higher PEG molecular weight. The exact reason behind such behavior of different PEG molecular weights is not very clear at the moment. However, it might be related to the formation of metal complexes. It has been reported that metal complexation would stabilize the metal ions against reduction [45]. Based on this assumption, the coordination of Pd(II) ions is probably more effective in lower PEG molecular weight, which in turn may inhibit the electron transfer necessary for the reduction process. Thus, a larger PEG chain length is preferred for maximum rate of Pd(II) reduction.
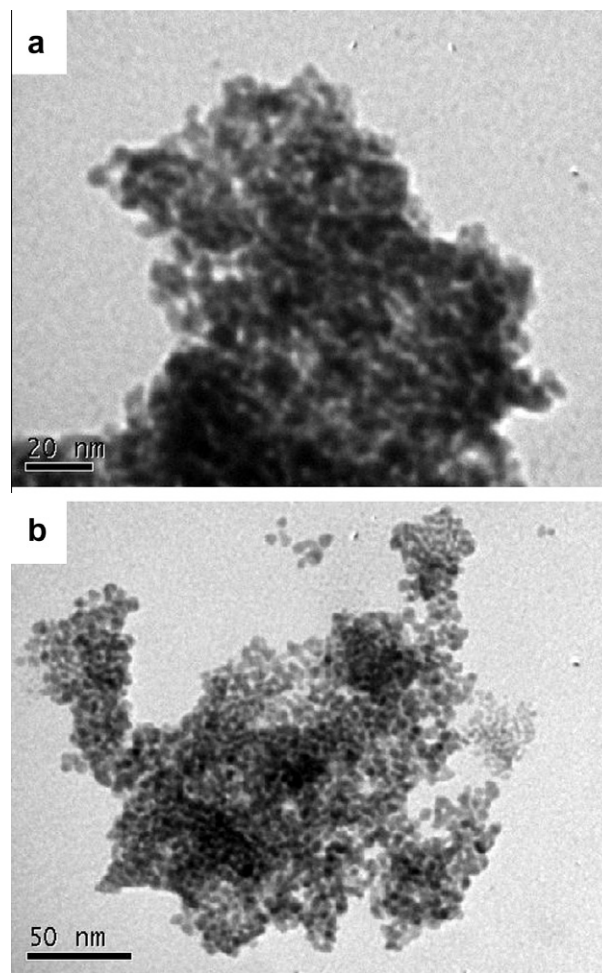

Fig. 5. TEM images of Pd nanoparticles prepared in different PEG molecular weights at 75 °C with 3.75 wt.% of Pd/PEG for 2 h: PEG2000 (a) and PEG6000 (b).

3.3. Catalytic performance

3.3.1. Hydrogenation of styrene

The catalytic activity of as-synthesized Pd nanoparticles in PEG4000 was firstly investigated using styrene hydrogenation as a model catalytic reaction in a 1 mmol biphenyl as a standard and 20 ml ethanol as a solvent at room temperature in a hydrogen atmosphere (Scheme 1). Fig. 6 illustrates the% conversion of reaction in Scheme 1 for different concentrations of styrene, mainly 0.5, 1, 1.5, 2, and 2.5 mmol at room temperature using the same weight of 25 mg catalyst for 90 min duration. The catalyst demonstrated superior activity at concentration ⩽1.5 mmol styrene; complete conversion (100%) of styrene to ethylbenzene product was achieved after 90 min at room temperature. At higher concentration of styrene, the% conversion decreased to 80% and
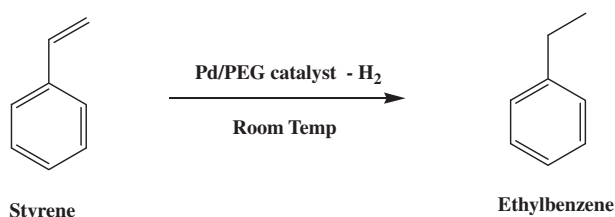
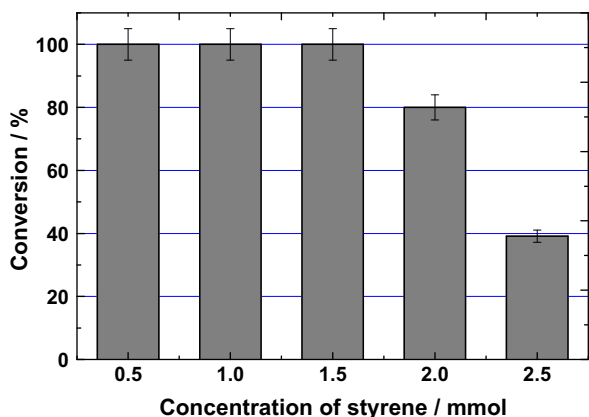**Scheme 1.** Hydrogenation of styrene with Pd/PEG catalyst.

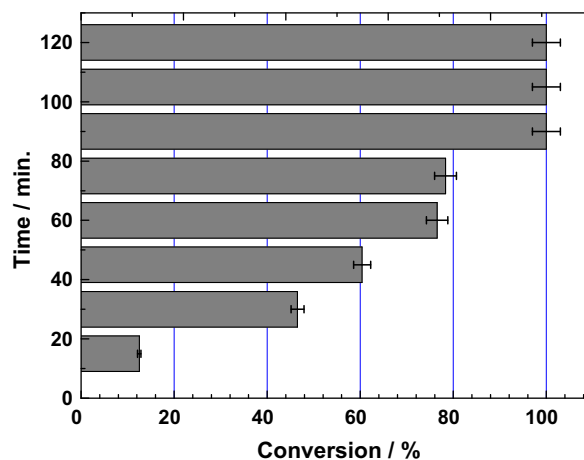**Fig. 6.** Effect of styrene concentration on the hydrogenation of styrene using Pd/PEG4000 catalyst.

Fig. 7. Effect of reaction time on styrene hydrogenation using Pd/PEG4000 catalyst.

39% using 2 and 2.5 mmol concentrations, respectively. Under the current experimental conditions, the complete conversion to ethylbenzene was achieved after 90 min, while a 78% conversion was obtained after 75 min. Further decrease in reaction time led to a gradual decrease in the% conversion as shown in Fig. 7. At shorter reaction time of 15 min, only 13% conversion was detected.

Determination of the minimum concentration of catalyst necessary for full conversion of styrene is indispensable step in optimizing the hydrogenation reaction. Different weights of Pd/PEG catalyst, mainly 150, 100, 50, 25, 19, and 13 mg in 20 ml of ethanol solvent, 1.5 mmol styrene under hydrogen atmosphere at room temperature were accordingly utilized. The results of styrene conversion%, ethylbenzene product selectivity% and the values of turnover frequency (TOF), calculated as the number of moles of product per mol of Pd per h are summarized in Table 4. At smaller weight of catalyst, 13 mg, only 10% conversion of styrene was obtained after 90 min, in comparison with 60% for using 19 mg catalyst for the same time. With a moderate catalyst weight of 25 mg, the hydrogenation reaction was completed after 90 min at room temperature, affording 100% styrene conversion to ethylbenzene with 100% selectivity. Interestingly, the selectivity to the desired product, ethylbenzene, was always 100% over the whole conversion range of 10–100%. The selectivity of the present catalyst system is mainly ascribed to the nanoparticles size of Pd and the nature of Pd metal itself. This result demonstrates a remarkable catalytic activity of Pd nanoparticles stabilized in PEG4000 toward styrene hydrogenation with a turnover number (TON: moles of

product per moles of Pd) of 990 and TOF of 660 h^{-1} (Entry 4 of Table 4). This TON is actually twice higher than a previously reported value of (TON = 448) achieved for hydrogenation of styrene using 1,10-phynanthroline-stabilized Pd nanoparticles in PEG [39]. The reported particle size of phynanthroline-stabilized Pd nanoparticles dispersed in PEG matrix was 2–6 nm size, and thus cannot explain the different catalytic performance of their catalyst and the Pd/PEG catalyst of the present work. A possible explanation for this is likely attributed to the presence of phynanthroline that could induce some surface deactivation for Pd nanoparticles by sterically hindering the diffusion of reactants toward the active sites of catalyst and eventually led to a lower catalytic activity in comparison with the present work.

We carried out a few control experiments to gain a better understanding of the hydrogenation reaction of styrene. Control experiments in absence of Pd failed to give any activity. Pd nanoparticles were then extracted from the Pd/PEG catalyst by dissolving the catalyst in pure water, followed by filtration to separate the Pd nanoparticles. The hydrogenation reaction of styrene was conducted in presence of as-extracted Pd nanoparticles with no PEG matrix. A conversion of 14% of styrene to ethylbenzene was obtained compared to 100% conversion in case of using Pd/PEG4000 under the same experimental conditions (Entry 4 of Table 4). This result suggests that the presence of PEG matrix is essential, which could act as a mobile supporting phase thereby giving higher stability and consequently enhancing the catalytic activity of Pd nanoparticles.

Table 4
Pd nanoparicles in PEG for the hydrogenation of styrene[a] and nitrobenzene[b].

Entry	Substrate	Product	Catalyst weight (mg)	Time (min)	Substrate conversion (%)	Product selectivity (%)	TOF (h^{-1})
1	Styrene	Ethylbenzene	150	90	100	100	126
2	Styrene	Ethylbenzene	100	90	100	100	178
3	Styrene	Ethylbenzene	50	90	100	100	322
4	Styrene	Ethylbenzene	25	90	100	100	660
5	Styrene	Ethylbenzene	19	90	60	100	385
6	Styrene	Ethylbenzene	13	90	10	100	189
7	Nitrobenzene	Aniline	100	180	100	100	83
8	Nitrobenzene	Aniline	50	180	84	91	126
9	Nitrobenzene	Aniline	25	180	41	83	90
10	Nitrobenzene	Aniline	13	180	16	71	73
11	Nitrobenzene	Aniline	100	120	93	93	71
12	Nitrobenzene	Aniline	100	90	42	86	32
13	Nitrobenzene	Aniline	100	60	22	87	18

TOF: turnover frequency calculated as the number of moles of product per mol of Pd per h.
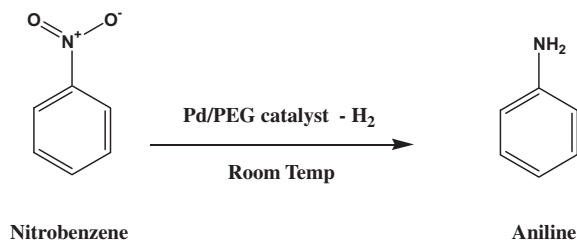[a] Reaction conditions: 1.5 mmol styrene, stirring, H$_2$ balloon, room temperature.
[b] Reaction conditions: 1 mmol nitrobenzene, stirring, H$_2$ balloon, room temperature.
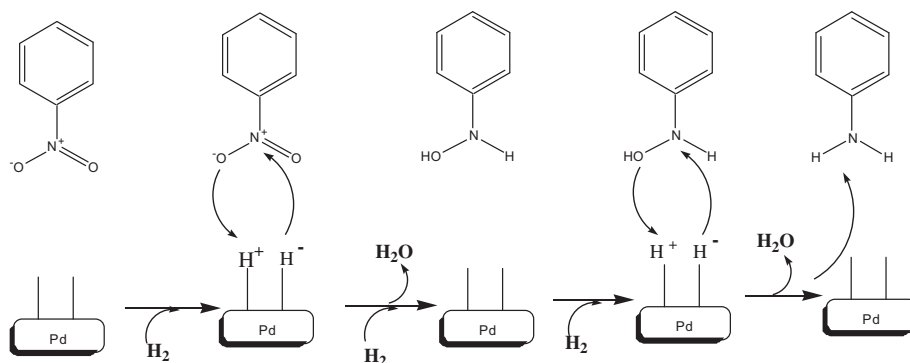
3.3.2. Reduction of nitrobenzene

To extend the application of the Pd/PEG catalyst to the hydrogenation of aromatic nitro compound, we examined its catalytic performance for the reduction of nitrobenzene to convert it to aniline. The reduction reaction was evaluated using Pd/PEG4000 catalyst in a liquid phase composed of 1 mmol biphenyl and 20 ml of ethanol at room temperature in a hydrogen atmosphere (Scheme 2). For those experiments, we chose first to apply the optimum conditions achieved during the hydrogenation of styrene (1.5 mmol target, 25 mg (3.75 wt.%) Pd/PEG4000 catalyst, 1.5 h, room temperature) for the reduction reaction of nitrobenzene. However, this experiment showed that Pd/PEG has almost no activity: extremely low% conversion of nitrobenzene (3%) to aniline was obtained. This means that under identical experimental conditions, the hydrogenation of styrene over Pd/PEG catalyst is much easier and faster compared to the reduction of nitrobenzene. We then changed the nitrobenzene concentration, catalyst weight, and reaction time to define the optimum levels necessary to achieve efficient catalytic performance of Pd/PEG catalyst for the reaction described in Scheme 2.

The% conversion of nitrobenzene to aniline was investigated using different concentrations of nitrobenzene, mainly 1, 1.5, and 2 mmol at room temperature using 100 mg catalyst for 180 min. With 1 mmol nitrobenzene, the catalyst showed 100% yield of aniline. While at higher nitrobenzene concentrations of 1.5 and 2 mmol, sharp decrease in% conversion was detected: the catalyst yields the product with only 57% and 40% conversion, respectively.

The dependence of conversion%, selectivity% of aniline, and values of calculated TOF on different reaction times and catalyst weights is presented in Table 4. As can be seen, under the present conditions, the as-prepared Pd/PEG catalyst is effective to completely convert 1 mmol nitrobenzene to aniline within 180 min at room temperature with 100% selectivity. By decreasing the reaction time, a conversion of 93% was obtained after 120 min. With further decrease in reaction time, a significant decrease in the% conversion was observed: 42% conversion after 90 min and only 22% after 60 min. The observed increase in nitrobenzene conver-

sion% with time since the beginning of the catalytic reaction clearly indicates that the Pd nanoparticles are well stabilized by PEG matrix.

The effect of using different Pd/PEG concentrations on the catalytic hydrogenation of nitrobenzene is also listed in Table 4. As a general trend, the% conversion was found to increase with an increase in catalyst weight. Only 16% conversion of nitrobenzene was achieved using 13 mg catalyst, in comparison with 41% obtained at a doubled weight of 25 mg catalyst. With a catalyst weight of 50 mg, the hydrogenation reaction reached 84%, whereas a full conversion of nitrobenzene to pure aniline with 100% selectivity was observed at 100 mg catalyst (Entry 7 of Table 4). It should be noted that controls using analogous samples without Pd showed no catalytic activity toward the conversion to aniline. The above results indicate that the Pd nanoparticles stabilized in PEG could exhibit a remarkable catalytic performance for the reduction of nitrobenzene producing aniline with 100% yield with a good TOF value of 83 h^{-1}. In addition, the product extraction from the current catalytic system is extremely facile, which offers the possibility for catalyst recycling as addressed in the following section.

The reaction mechanism for the reduction of nitrobenzene to aniline has been reported by a group of authors [46–49]. They indicated that the hydrogenation reaction may proceed via successive steps, which can be simply written as follows:

$$C_6H_5-NO_2 \rightarrow C_6H_5-NO \rightarrow C_6H_5-NHOH \rightarrow C_6H_5-NH_2$$
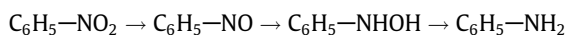
In another possible mechanism proposed by Gelder et al. [50], the hydrogenation reaction may take place through the formation of nitrosobenzene as an intermediate according to the following form:

$$C_6H_5-NO_2 \rightarrow [C_6H_5-NOH(ads)] \rightarrow C_6H_5-NHOH \rightarrow C_6H_5-NH_2$$
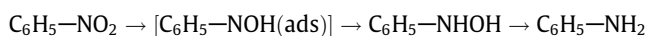
where $[C_6H_5-NOH(ads)]$ is the adsorbed species. As shown, phenylhydroxylamine/ C_6H_5-NHOH, is an intermediate in both mechanisms. It has been reported that the accumulation of this hazardous intermediate is undesirable as it may lead to rapid exothermic decomposition and/or formation of condensation products during the hydrogenation of nitrobenzene [48,51]. In view of the consideration mentioned above, a proposed mechanism of the reduction of nitrobenzene using the current Pd/PEG catalyst involving phenylhydroxylamine intermediate can be schematically depicted in Scheme 3.

3.3.3. Recycling of the Pd/PEG catalyst

In heterogeneous catalysis, it is essential, indispensable practical step to release and recover the catalyst from the reaction medium and reuse it for subsequent reaction cycles until the catalyst showed inactivity. Accordingly, to test the catalyst lifetime, the ability to recycle the Pd/PEG catalyst was studied for the hydroge-
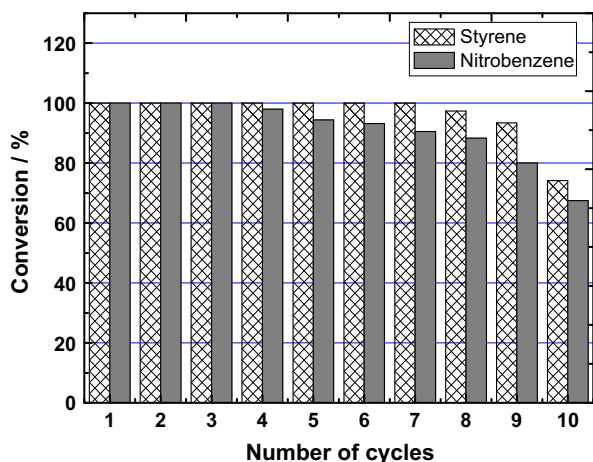

Scheme 2. Reduction of nitrobenzene with Pd/PEG catalyst.

Scheme 3. Proposed mechanism for the Pd/PEG-catalyzed hydrogenation of nitrobenzene.

Fig. 8. Recycling of Pd/PEG4000 catalyst used for hydrogenation of styrene and nitrobenzene.

nation reactions of styrene and nitrobenzene. After each reaction run, the organic products were extracted into diethyl ether followed by simple decantation. The ether-immiscible PEG layer containing Pd nanoparticles catalyst was recovered and reused with fresh reaction mixture in a subsequent run; photographs of Supporting information (Fig. S1) show the recycling procedure. The results of recycling uses of Pd/PEG catalyst for hydrogenation of styrene and nitrobenzene are presented in Fig. 8. The Pd/PEG catalyst could be successfully recycled for seven times for styrene hydrogenation without any loss in activity, giving 100% conversion to ethylbenzene. The catalyst activity slightly dropped in runs 8 and 9, yielding 97% and 93% conversions, respectively. In the 10th run, the catalyst showed 74% conversion. The deactivation of the Pd/PEG catalyst is likely related to the formation of aggregated Pd nanoparticles, which led to a decrease in the surface area of the catalyst.

Similarly, the recyclability of Pd/PEG catalyst was also examined for the reduction of nitrobenzene to aniline. In this case, complete conversions were achieved in the runs 1–3 as illustrated in Fig. 8. The catalytic activity was then slightly dropped in the 4th run yielding 98% conversion. The activity was further decreased to 90% in run 7. A gradual decrease in activity was observed again in runs 8–10 where conversions of 88%, 80%, and 67% were obtained, respectively. As explained above, the agglomeration of Pd nanoparticles is likely to take place which in turn led to the deactivation of Pd/PEG catalyst during the recycling procedure.

Based on the above observations, the catalyst recyclability was more efficient in case of styrene hydrogenation compared to the reduction of nitrobenzene. The main reason may be related to the different degrees of Pd aggregation in both reactions. In addition, the different leaching behavior of Pd nanoparticles from catalyst into the reaction medium in both cases may be another reason. The leaching of active species of catalyst is often a serious problem for supported metal catalysts, which leads to catalyst depletion and causes difficulty in catalyst separation and recycling. Previous reports on Heck reaction catalyzed by supported Pd nanoparticles indicated that the Pd leaching process is essentially dependent on different factors including the solvent, base, substrate and product, and the surface nature of support [52–54]. We examined the leaching behavior of Pd/PEG catalyst for both reactions. The Pd content was determined in the extracted solutions using ICP-OES. Undetectable levels for Pd leaching (our ICP-OES detection limit for Pd = 0.04 ppm) were obtained for both reaction solutions, indicating extremely low degree of Pd leaching under the current experimental conditions. In addition, we did not

observe any further increase in reactivity (conversion efficiency) after the removal of the supported Pd nanoparticles from the reaction medium. This means that the leached Pd, even if occurred, has nothing to do with the catalytic hydrogenation reactions, indicating again that the hydrogenation reactions most probably proceed heterogeneously. In addition, this observation suggests that Pd leaching is not the direct reason behind the reduction in catalytic activity during the catalyst recycling.

Another important piece of information concerning the practical use of heterogeneous catalyst is its storage stability. Generally, the storage of supported Pd nanoparticles leads to a decrease in catalytic activity, due to the oxygenation of Pd nanoparticles in air [21,55]. Interestingly, the Pd/PEG catalyst prepared in this work exhibits excellent storage stability for 3 months even upon exposure to air, and thus no special care is required for its storage. This actually indicates that Pd nanoparticles in PEG are stable enough to retain high catalytic activity in recycling as well as during storage. Encouraged by these promising results, further studies to utilize this Pd/PEG catalyst system in other heterogeneous catalytic reactions, including the hydrogenation of crotonaldehyde, the oxidation of benzene, and the oxidative desulfurization of fuel are in progress in our laboratories.

4. Conclusion

A heterogeneous Pd(0) nanoparticles catalyst was successively synthesized by simple, mild, and efficient chemical approach using PEG as stabilizer with no additional reducing agent. The XRD and TEM analysis confirmed the presence of highly dispersed Pd(0) nanoparticles in PEG with small average particle size distribution of 5 nm. The as-synthesized Pd/PEG catalyst exhibited an outstanding catalytic activity and selectivity for the hydrogenation of styrene and nitrobenzene under mild conditions in an environmentally friendly solvent system. The catalytic performance is markedly dependent on catalyst and target concentrations and reaction time. Importantly, the catalysts demonstrated excellent stability for easily removal from the reaction mixture and could be reused for seven times for styrene and three times in case of nitrobenzene with no loss in activity. No Pd leaching was detected on examined samples during or after their use over ten reaction cycles for both styrene and nitrobenzene, indicating the good stabilizing effect of PEG for Pd nanoparticles. Extending the scope of applications, this catalyst is expected to demonstrate a broad range of utility for other heterogeneous catalytic reactions, which is being underway.

Appendix A. Supplementary material

Supplementary data associated with this article can be found, in the online version, at doi:10.1016/j.jcat.2011.11.001.

References

[1] J.S. Bradley, in: G. Schmid (Ed.), Clusters and Colloids: From Theory to Application, VCH, New York, 1994, p. 459.
[2] D.V. Goia, E. Matijevic, New J. Chem. 22 (1998) 1203.
[3] C.N.R. Rao, G.U. Kulkarni, P.J. Thomas, P.P. Edwards, Chem. Soc. Rev. 28 (2000) 27.
[4] S.A. Maier, M.L. Brongersma, P.G. Kik, S. Meltzer, A.G. Requicha, H.A. Atwater, Adv. Mater. 13 (2001) 1501.
[5] C.B. Murray, S. Sun, H. Doyle, T. Betley, Mater Res. Soc. Bull. 26 (2001) 985.
[6] M.P. Pileni, Adv. Funct. Mater. 11 (2001) 323.
[7] P.V. Kamat, J. Phys. Chem. B 106 (2002) 7729.
[8] R.G. Finke, in: D.L. Feldheim, C.A. Foss Jr. (Eds.), Metal Nanoparticles: Synthesis, Characterization and Applications, Foss, Marcel Dekker, New York, 2002, p. 17. Chapter 2.
[9] T.S. Huang, Y.H. Wang, J.Y. Jiang, Z. Lin Jin, Chin. Chem. Lett. 19 (2008) 102.
[10] C.P. Mehnert, J.Y. Ying, Chem. Commun. (1997) 2215.
[11] C.P. Mehnert, D.W. Weaver, J.Y. Ying, J. Am. Chem. Soc. 120 (1998) 12289.

[12] M.T. Reetz, R. Breinbauerm, K. Wanniger, Tetrahedron Lett. 37 (1996) 4499.
[13] M.T. Reetz, E. Westermann, Angew. Chem. Int. Ed. 39 (2000) 165.
[14] K.R. Gopidas, J.K. Whitesell, M.A. Fox, Nano Lett. 3 (2003) 1757.
[15] L.K. Yeung, R.M. Crooks, Nano Lett. 1 (2001) 14.
[16] R.R. Deshmukh, R. Rajagopal, K.V. Srinivaan, Chem. Commun. (2001) 1544.
[17] N.A. Hamill, C. Hardacre, S.E.J. McMath, Green Chem. 4 (2002) 139.
[18] S. Klingelhöfer, W. Heitz, A. Greiner, S. Östereich, S. Förster, M. Antonietti, J. Am. Chem. Soc. 119 (1997) 10116.
[19] S. Pathak, M.T. Greci, R.C. Kwong, K. Mercado, G.K.S. Prakash, G.A. Olah, M.E. Thompson, Chem. Mater. 12 (2000) 1985.
[20] Ali R. Siamaki, Abd El Rahman S. Khder, Victor Abdelsayed, M. Samy El-Shall, B. Frank Gupton, J. Catal. 279 (2011) 1.
[21] Hao Wu, Liangming Zhuo, Qiang He, Xuepin Liao, Bi Shi, Appl. Catal. A: Gen. 366 (2009) 44.
[22] P. Sangeetha, K. Shanthi, K.S. Rama Rao, B. Viswanathan, P. Selvam, Appl. Catal. A: Gen. 353 (2009) 160.
[23] Sonia Domínguez-Domínguez, Ángel Berenguer-Murcia, Ángel Linares-Solano, Diego Cazorla-Amorós, J. Catal. 257 (2008) 87.
[24] J. Silvestre-Albero, F. Rodríguez-Reinoso, A. Sepúlveda-Escribano, J. Catal. 210 (2002) 127.
[25] Y.T. Vu, J.E. Mark, Coll. Polym. Sci. 282 (2004) 613.
[26] C.C. Luo, Y.H. Zhang, Y.G. Wang, J. Mol. Catal. A: Chem. 229 (2005) 7.
[27] X. Ma, T. Jiang, B. Han, J. Zhang, S. Miao, K. Ding, G. An, Y. Xie, Y. Zhou, A. Zhu, Catal. Comm. 9 (2008) 70.
[28] D. de Caro, J.S. Bradley, Chem. Mater. 14 (1998) 245.
[29] D.-J. Guo, H.-L. Li, Electrochem. Commun. 6 (2004) 999.
[30] F.A. Harraz, S.M. El-Sheikh, R.M. Mohamed, I.A. Ibrahim, Int. J. Nanoparticles 2 (1/2/3/4/5/6) (2009) 361.
[31] Avelino Corma, Hermenegildo García, Antonio Leyva, Tetrahedron 61 (2005) 9848.
[32] Avelino Corma, Hermenegildo García, Antonio Leyva, J. Catal. 240 (2006) 87.
[33] Wei Han, Ning Liu, Chun Liu, Zi Lin Jin, Chin. Chem. Lett. 21 (2010) 1411.
[34] Andréa Luzia F. de Souza, Lucyane C. da Silva, Bianca L. Oliveira, O.A.C. Antunes, Tetrahedron Lett. 49 (2008) 3895.
[35] Liang Yin, Zhan-hui Zhang, Yong-mei Wang, Tetrahedron 62 (2006) 9359.
[36] Bo Feng, Li Hua, Zhenshan Hou, Hanmin Yang, Yu Hu, Huan Li, Xiuge Zhao, Catal. Commun. 10 (2009) 1542.
[37] Patrice Ribiere, Valerie Declerck, Yannig Nedellec, Neerja Yadav-Bhatnagar, Jean Martinez, Frederic Lamaty, Tetrahedron 62 (2006) 10456.
[38] Vadapalli Chandrasekhar, Ramakirushnan Suriya Narayanan, Tetrahedron Lett. 52 (2011) 3527.
[39] Unnikrishnan R. Pillai, Endalkachew Sahle-Demessie, J. Mol. Catal. A: Chem. 222 (2004) 153.
[40] Xiumin Ma, Tao Jiang, Buxing Han, Jicheng Zhang, Shiding Miao, Kunlun Ding, Guimin An, Ye Xie, Yinxi Zhou, Anlian Zhu, Catal. Commun. 9 (2008) 70.
[41] Xiangchun Meng, Haiyang Cheng, Yoshinari Akiyama, Yufen Hao, Weibin Qiao, Yancun Yu, Fengyu Zhao, Shin-ichiro Fujita, Masahiko Arai, J. Catal. 264 (2009) 1.
[42] P. Ahmadian Namini, A.A. Babaluo, B. Bayati, Int. J. Nanosci. Nanotechnol. 3 (2007) 37.
[43] B.P.S. Chauhan, R. Sardar, U. Latif, M. Chauhan, W.J. Lamoreaux, Acta Chim. Solv. 52 (2005) 361.
[44] C.B. Rodella, P.A.P. Nascente, V.R. Masteralo, R.W.A. Franco, C.J. Magon, A.O. Florentino, Phys. Status Solidi (A) 187 (2001) 161.
[45] F. Bonet, C. Guery, D. Guyomard, R.H. Urbina, K. Tekaia-Elhsissen, J.-M. Tarascon, Solid State Ionics 126 (1999) 337.
[46] H. Li, Q. Zhao, Y. Wan, W. Dai, M. Qiao, J. Catal. 244 (2006) 251.
[47] H.D. Burge, D.J. Collins, B.H. Davis, Ind. Eng. Chem. Prod. Res. Dev. 19 (1980) 389.
[48] N. Mahata, A.F. Cunha, J.J.M. Órfão, J.L. Figueiredo, Appl. Catal. A: Gen. 351 (2008) 204.
[49] K. Shimizu, Y. Miyamoto, A. Satsuma, J. Catal. 270 (2010) 86.
[50] E.A. Gelder, S.D. Jackson, C.M. Lok, Chem. Commun. (2005) 522.
[51] P. Baumeister, H.-U. Blaser, M. Studer, Catal. Lett. 49 (1997) 219.
[52] F.Y. Zhao, M. Shirai, Y. Ikushima, M. Arai, J. Mol. Catal. A: Chem. 180 (2002) 211.
[53] R.G. Heidenreich, J.G.E. Krauter, J. Pietseh, K. Kohler, J. Mol. Catal. A: Chem. 182/183 (2002) 499.
[54] A. Biffis, M. Zecca, M. Basato, Eur. J. Inorg. Chem. (2001) 1131.
[55] Y.J. Jiang, Q.M. Gao, J. Am. Chem. Soc. 128 (2006) 716.